



# A novel fibrinogen $\gamma$ -chain frameshift mutation, p. Cys365Phefs\*41, causing hypofibrinogenemia with bleeding phenotype in a Chinese family

Weijie Zhou<sup>1,2,3,4#</sup>, Yan Huang<sup>5#</sup>, Jie Wei<sup>5#</sup>, Jun Li Wang<sup>3</sup>, Boming Huang<sup>4</sup>, Xiaoxuan Zhou<sup>4</sup>, Jie Yan<sup>6</sup>, Yangyang Wu<sup>6</sup>, Faquan Lin<sup>6</sup>, Wangrong Wen<sup>1,2</sup>

<sup>1</sup>Clinical Laboratory, The Affiliated Shunde Hospital of Jinan University, Foshan, China; <sup>2</sup>Clinical Laboratory Center, The First Affiliated Hospital of Jinan University, Guangzhou, China; <sup>3</sup>Reproductive Genetics Laboratory, Affiliated Hospital of Youjiang Medical University for Nationalities, Baise, China; <sup>4</sup>Clinical Laboratory, The People's Hospital of Baise, Baise, China; <sup>5</sup>Department of Hematology, The People's Hospital of Baise, Baise, China; <sup>6</sup>Clinical Laboratory, The Affiliated Hospital of Guangxi Medical University, Nanning, China

**Contributions:** (I) Conception and design: Y Huang, J Yan; (II) Administrative support: J Wei, W Zhou; (III) Provision of study materials or patients: W Zhou, Y Huang; (IV) Collection and assembly of data: W Zhou, B Huang, X Zhou, Y Wu; (V) Data analysis and interpretation: W Zhou, B Huang, X Zhou, Y Wu; (VI) Manuscript writing: All authors; (VII) Final approval of manuscript: All authors.

<sup>#</sup>These authors contributed equally to this work.

**Correspondence to:** Wangrong Wen. Clinical Laboratory, The Affiliated Shunde Hospital of Jinan University, Foshan 528305, China; Clinical Laboratory Center, The First Affiliated Hospital of Jinan University, Guangzhou, China. Email: wenwangrong@yeah.net; Faquan Lin. Clinical Laboratory, The Affiliated Hospital of Guangxi Medical University, Nanning, China. Email: faquanlin@163.com.

**Background:** Congenital hypofibrinogenemia is a rare bleeding disease that is classified as the quantitative deficient type. In the present study, investigated the relationship between the genotype and phenotype in a family with hypofibrinogenemia.

**Methods:** The proband was aware of a predisposition to bleeding. Functional analysis was performed for her all family members, including coagulation function tests, thrombus molecular markers, thromboelastography, scanning electron microscopy, DNA sequencing, and high-performance liquid chromatography-mass spectrometry (HPLC-MS). Pathogenicity analysis and protein modeling of mutant amino acids were also performed.

**Results:** A novel heterozygous mutation in c.1094delG was detected in FGG exon 8, which resulted in p. Cys365Phefs\*41 (containing the signal peptide) in the proband and her mother, who showed a corresponding decrease in fibrinogen function and levels. Thromboelastography indicated that the strength of their blood clots decreased and they had an increased risk of bleeding. The proband fibrin network structure was looser than healthy controls, with large pores in the network, which increased the permeability of lytic enzymes. Results of HPLC-MS showed a lack of mutant peptide chain expression in their plasma, indicating that the family had congenital hypofibrinogenemia, with a clinical phenotype that is related to the degree of fibrinogen deficiency. The mutation truncated the  $\gamma$ -peptide chain and destroyed the functional structure of fibrinogen, including the  $\gamma$ 352Cys- $\gamma$ 365Cys disulfide bond. The truncated peptide chains may also lead to nonsense-mediated decay.

**Conclusions:** The mutation induced a structural change at the carboxyl-terminal of the fibrinogen molecule, leading to fibrinogen secretion dysfunction.

**Keywords:** Hypofibrinogenemia; pathogenicity analysis; protein modeling; functional analysis; bleeding phenotype

Submitted Jun 02, 2021. Accepted for publication Aug 05, 2021.

doi: 10.21037/atm-21-3207

View this article at: <https://dx.doi.org/10.21037/atm-21-3207>

## Introduction

According to the International Society of Thrombosis and Haemostasis (ISTH) Fibrinogen Mutation Database, there have been several reports of disulfide bond disruption and molecular functional structure destruction caused by mutations (<http://site.geht.org/base-de-donnees-fibrinogene/>). Congenital fibrinogen disorder (CFD) is an inherited disease with fibrinogen gene defects leading to structural abnormalities and functional defects with fibrinogen. Most diseases are autosomal dominant, while a few are autosomal recessive. Based on different molecular pathogenic mechanisms, CFD can be divided into the following 2 types: quantity defect (caused by afibrinogenemia or hypofibrinogenemia) and quality defects (caused by dysfibrinogenemia or hypofibrinogenemia). Worldwide, the incidence of autosomal recessive CFD is about 1/106 in some European and North and South America, and autosomal dominant inheritance is 11/103, but the actual incidence is believed to be higher (1,2).

The fibrinogen gene is located in a region of chromosome 4, is about 50 kb in size, and produces the fibrinogen protein in the liver, which is then secreted into circulation. The fibrinogen molecule is composed of 2 groups of 3 peptides ( $\text{A}\alpha$ ,  $\text{B}\beta$  and  $\gamma$ ) encoded by *FGA*, *FGB*, and *FGG* genes, respectively (3). Twenty-nine interchain and intrachain disulfide bonds connect the different parts of the structure; these are critical for the synthesis, secretion, stability, and biological function of fibrinogen (4). The molecule is a slender, jointed, rod-shaped triplet with a smaller center known as the E domain; the more significant parts at both ends are known as the D-domains (5). The E and D-domains contain molecular functional structures which are involved in all stages of fibrinogen conversion to fibrin (6). These include the fibrinogen intermolecular binding sites, holes a and b in the D-domain, a calcium-binding site in the D-domain, a thrombin-binding site in the E domain, as well as intermolecular aggregation sites of fibrin in the E domain referred to as knobs (7). These are exposed by the action of thrombin and combine with the holes to form the E:D structure. The D-domain between adjacent fibrinogen molecules can connect to form the D:D structure (8,9). These two structures are semi-staggered and interact to form double-stranded fibrin filaments of specific period lengths. When activated, the filaments thicken to form the final 3D network structure and fulfills the physiological function of fibrinogen.

We recently identified a new hemorrhagic phenotype

of congenital hypofibrinogenemia. DNA sequencing revealed heterozygous mutations in c. 1094delG was detected in FGG exon 8, resulting in p. Cys365Phefs\*41 (which contains the signaling peptide) in a proband and her mother. The occurrence of bleeding events in family members was related to the degree of fibrinogen deficiency. This fibrinogen mutation has not been previously reported. We present the following article in accordance with the MDAR reporting checklist (available at <https://dx.doi.org/10.21037/atm-21-3207>).

## Methods

### Sample collection

Peripheral blood samples were taken from 4 family members. An automated hematology analyzer (ACL-TOP 700; Instrument Laboratory Company, Bedford, MA, USA) was used to determine the levels of D-dimer, fibrinogen and fibrin degradation products (FDP), prothrombin time (PT), activated partial thromboplastin time (APTT), thrombin time (TT), and fibrinogen (using Clauss test and the prothrombin derivative method). The level of fibrinogen antigen was determined by human fibrinogen enzyme-linked immunosorbent assay (ELISA) kit (Kusabio, Wuhan, China). Thrombin-antithrombin complex (TAT),  $\alpha$ 2-plasmininhibitor-plasmin complex (PIC), tissue plasminogen activator-inhibitor complex (tPAIC), and thrombomodulin (TM) were measured via qualitative chemiluminescence enzyme immunoassay performed on HISCL automated analyzers (HISCL-2000i; Sysmex, Kobe, Japan).

### Clot waveform analysis (CWA)

All CWA were performed using an ACL TOP 700 (Instrument Laboratory Company, Bedford, MA, USA), which uses a turbidimetric method for clot detection. The results were digitized in OriginPro 2019B (OriginLab Corporation, Northampton, Massachusetts, USA). We investigated the dynamics of the formation of fibrin for this family, including a record of the maximum velocity of clot formation (first derivative, expressed as mAbs/s), the maximum acceleration of clot formation (second derivative, expressed as mAbs/s<sup>2</sup>), the amplitude of the coagulation curve (delta, expressed as mAbs) that is obtained from the difference between the maximum and the minimum absorbance points (10), and the time to reach the threshold, which is the algorithm used for the Clauss fibrinogen assay

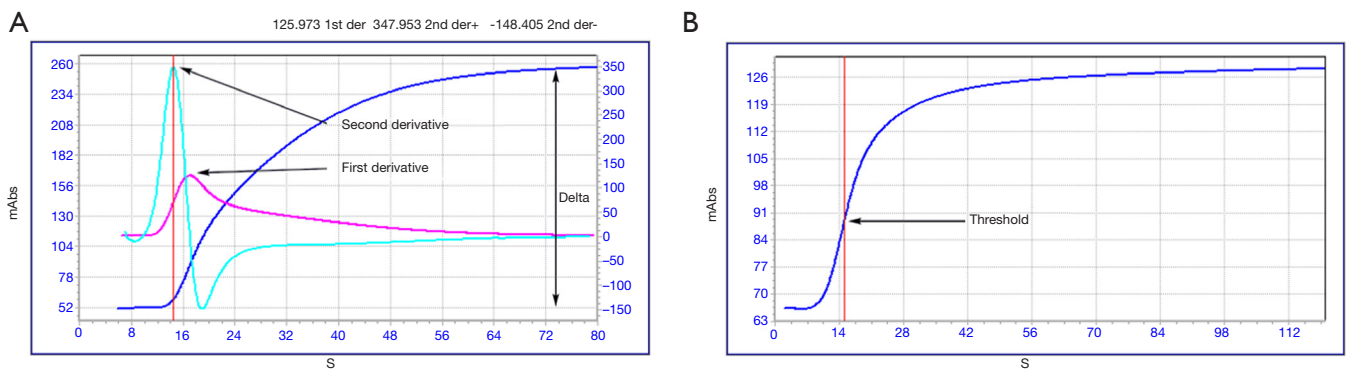


**Figure 1** Clot waveform analysis in a healthy control. (A) Arrows indicate the first derivative (expressed as mAbs/s) and the second derivative (expressed as mAbs/s<sup>2</sup>), respectively. Amplitude of each coagulation curve (delta, expressed as mAbs) is indicated by the double arrow. (B) Arrow indicates the threshold, and the X-axis is the reaction time. Intersection of the red line on the X-axis is the time needed to reach the threshold.

determination (*Figure 1*).

#### ***Fibrinogen purification and isolation***

The Fibrinogen of proband and normal individuals were obtained from citrate-anticoagulated plasma, and the samples were used 25% saturated ammonium sulfate solution. The bicinchoninic acid assay was used to measure the fibrinogen concentration. The fibrinogen extract obtained was subjected to sodium dodecylsulfate-polyacrylamide gel electrophoresis (SDS-PAGE) on a 10% resolving gel. Following Coomassie Brilliant Blue staining, the sample was decolorized and photographed.

#### ***Polymerase chain reaction (PCR) and DNA sequencing***

And the genomic DNA of four family members were extracted via extraction kit (Tiangen Biotechnology, Beijing, China). The reaction mixture of FGA, FGB, and FGG, was amplified in 50  $\mu$ L reaction mixture that including template DNA, forward primer, reverse primer, EmeraldAmp PCR maternal mixture (premixed twice) (Takala, Dalian, China), and ribonuclease water. The initial denaturation temperature was 95  $^{\circ}$ C, the amplification time was 5 min, the denaturation temperature was 94  $^{\circ}$ C, the amplification period was 30 s at 55  $^{\circ}$ C and the amplification time was 30 s (except for the second and fifth primers of FGB, which were 54  $^{\circ}$ C), the amplification time was 45 s in the temperature 72  $^{\circ}$ C. The PCR products were conducted bidirectionally via using the standard Sanger dideoxy terminator sequence

on the ABI 3730XL sequencer (Applied Biosystems, Foster City, CA, USA).

#### ***High-performance liquid chromatography-mass spectrometry (HPLC-MS)***

The samples were stained by SDS-PAGE electrophoresis and Coomassie Brilliant Blue R250 staining. The target protein was removed from the gel, washed twice with double-distilled water, and placed in a clean Eppendorf (EP) tube. The protein was washed several times with 50% ethanol to remove the stain. The protein was washed twice with double-distilled water, then dehydrated with 100% acetonitrile and vacuum dried. A reduction reaction was subsequently performed by incubation with 10 mM dithiothreitol (1 M of stored liquid was diluted with 50 mM NH<sub>4</sub>HCO<sub>3</sub>) at 55  $^{\circ}$ C for 30–45 min. ACN was used again for dehydration and vacuum drying; 55 mM iodoacetamide was added to alkylate the mixture at room temperature without light for 45 min. The sample was washed with double-distilled water and then dehydrated with ACN twice and vacuum dried for 10 min. Then 10 ng/ $\mu$ L trypsin was incubated overnight at 37  $^{\circ}$ C for digestion. A matrix solution (50% ACN in 5% FA) was added, followed by oscillation of the sample. The liquid supernatant was removed and placed in a new EP tube, and the above process was repeated. Finally, the liquid was dried with a vacuum concentrator and dissolved in 20  $\mu$ L matrix solution. A 1  $\mu$ L sample was injected into a Q Exactive HF combined mass spectrometer (Thermo Fisher Scientific, San Jose, CA, USA) with an

analytical column gradient and eluted for identification.

### ***Pathogenicity analysis and protein modeling of mutant amino acids***

Using Mutation Taster (<http://www.mutationtaster.org/>) in the National Center for Biotechnology Information (NCBI) database, the mutant amino acid pathogenicity (Uniprot peptide ID: P02679, Ensembl transcript ID: ENST00000404648 and GenBank transcript ID: NM\_000509) was predicted. PhastCons and phyloP are both methods to determine the grade of conservation of a given nucleotide. PhastCons values can vary between 0 and 1, reflecting multiple alignments based on genomic sequences of 46 different species, and the probability that each nucleotide belongs to a conservative element (the closer the value is to 1). It considers not just each alignment column but also the flanking columns. PhyloP (values between -14 and +6) measures the conservatism of each column, ignoring the influence of its neighbors. Using the 3D structure of fibrinogen to generate its molecular structure (protein database: 3GHG; <http://www.rcsb.org/pdb/home/home.do>), the mutation site was modeled using the PyMol protein structure viewer (PyMol Molecular Graphics System; Schrödinger, New York, USA).

### ***Thromboelastography***

Thromboelastography (CFMS Lepu-8800; Beijing Lepu Medical Technology, Beijing, China) was used for thromboelastography within 2h after sample collection. All reagents were maintained at 37 °C before detection. Citrate-anticoagulated blood (1 mL) was added to a reagent bottle containing kaolin, and the contents were mixed by inversion of the bottle, followed by stationary incubation for 15 min. The reaction cup was placed in the test channel, and 20  $\mu$ L CaCl<sub>2</sub> was added to the bottom of the reaction cup. The reaction bottle was mixed by agitation, and subsequently, 340  $\mu$ L of whole blood was added to the cup along its upper edge.

### ***Scanning electron microscopy of fibrin clots***

Plasma (33  $\mu$ L) was incubated along with 1  $\mu$ L thrombin (final concentration: 2 or 3 U/mL) at 37 °C for washing three times with 0.1 M phosphate-buffered saline (PBS; pH 7.4). The sample was fixed at 4 °C (optimal) or room temperature for 2 h with 3% glutaraldehyde in PBS, followed by washing 3 times with PBS and dehydration

through a series of graded alcohol (30%, 50%, 70%, 80%, 90%, and 100%) for approximately 10 min at each grade. Dehydration by 80%, 90%, and 100% alcohol at 4 °C, 30%, 50%, and 70% ethanol and at room temperature. After that, the samples were dried in a critical point dryer and then observed directly or coated with metal, it was observed under a scanning electron microscope (Tescan, Brno, Czech Republic). The mean fiber diameter within the fibrinogen network was measured using Image-Pro Plus 6.0 software (Media Cybernetics company, Silver Springs, MD, USA).

### ***Statistical analysis***

Data were analyzed using SPSS 22.0 (SPSS, Chicago, IL, USA) software and are expressed as the mean  $\pm$  standard deviation. The means of two independent groups were compared by the independent samples *t*-test. All of the tests were two-sided, and P values less than 0.05 were regarded as statistically significant.

### ***Ethical statement***

All procedures performed in this study involving human participants were in accordance with the Declaration of Helsinki (as revised in 2013). The study was approved by the medical ethics committee at the First Affiliated Hospital of Guangxi Medical University, Nanning, Guangxi, China (No. 2020 KY-E-162) and informed consent was taken from all the patients.

## **Results**

### ***Patients***

The proband was a 26-year-old woman from Baise, a city located in the Guangxi Zhuang Autonomous Region of China. She had normal PT, APTT, and TT. Her fibrinogen levels were 1.17 g/L according to the Clauss assay, 1.67 g/L according to the PT-derived method, and 1.20 g/L according to ELISA. Her fibrinogen Clauss/PT-derived ratio was 0.70, suggesting decreased levels of fibrinogen antigen, as well as activity. The proband had been aware of a predisposition to bleeding, such as hypermenorrhea, gingival bleeding, and decreased wound healing capacity. Decreased fibrinogen levels were also observed in the proband's mother when measured by Clauss assay and ELISA, but using the PT-derived method, the levels appeared to be in the normal range.

**Table 1** Coagulation function analysis of the family members

Family member	PT (s)	APTT (s)	TT (s)	Fibrinogen (g/L)			
				Clauss assay	PT-derived method	Clauss/PT-derived ratio	ELISA
Father	10.5	33.6	14.5	2.67	2.80	0.95	2.90
Mother	11.3	32.5	17.7	1.61	2.24	0.72	1.78
Proband	12.3	37.0	19.8	1.17	1.67	0.70	1.20
Brother	13.0	33.0	16.2	2.18	2.53	0.86	2.60
Reference range	9–15	23–40	9–15	2–5	2–5		2–5

APTT, activated partial thromboplastin time; ELISA, enzyme-linked immunosorbent assay; PT, prothrombin time; TT, thrombin time.

**Table 2** Thrombus molecular biomarkers of the family members

Family member	D-dimer level (ng/mL)	FDP (µg/mL)	TAT (ng/mL)	PIC (µg/mL)	TM (TU/mL)	tPAIC (ng/mL)
Father	21.0	0.34	0.63	0.37	4.93	2.68
Mother	13.0	0.17	0.7	0.45	5.51	5.58
Proband	2.0	0.15	1.06	0.38	6.02	7.62
Brother	155.0	1.44	1.01	0.68	4.76	6.21
Reference range	<243.0	<5.0	<4	<0.8	3.8–13.3	<17

FDP, fibrin degradation products; PIC,  $\alpha$ 2-plasmininhibitor-plasmin complex; TAT, thrombin-antithrombin complex; TM, thrombomodulin; tPAIC, tissue plasminogen activator-inhibitor complex.

**Table 3** Coagulation factor activities of the family members

Family member	FVIII:C (%)	FIX:C (%)	FXI:C (%)	FXII:C (%)
Father	76.2	110.0	109.0	64.3
Mother	78.0	104.0	97.7	102.1
Proband	56.5	75.6	78.6	50.4
Reference range	50–150	50–150	65–150	50–150

FIX:C, coagulation factor IX activity; FXI:C, coagulation factor XI activity; FXII:C, coagulation factor XII activity; FVIII:C, coagulation factor VIII activity.

Additionally, the proband's father's and younger brother's coagulation functions were normal (*Table 1*). Thrombus molecular biomarkers, including D-dimer, FDP, TAT, PIC, tPAIC, and TM (*Table 2*), and coagulation factor activities, including VIII, IX, XI, and XII (*Table 3*), were normal in the family. The father, mother, and younger brother of the proband did not have a history of bleeding or thrombus.

### DNA sequencing

A novel heterozygous frameshift mutation in c.1094delG

was detected in FGG exon 8, resulting in p. Cys365Phefs\*41 (containing the signal peptide) in the proband and her mother. The mutation was retrieved from the fibrinogen mutation database (<http://site.geht.org/base-de-donnees-fibrinogene/>), and sequenced from 100 healthy individuals in order to exclude polymorphisms.

### SDS-PAGE analysis

Compared with fibrinogen derived from healthy controls, there was no difference in the relative molecular mass of

the 3 fibrinogen peptide chains ( $A\alpha$ ,  $B\beta$ , and  $\gamma$ ) between the proband and her family members (*Figure 2*).

### HPLC-MS

HPLC-MS showed a peak of representing a normal peptide (CHAGHLNGVYY), with no indication of an abnormal peptide (FTLAISMFEITK) that would correspond to a variant  $\gamma$ -chain. This indicated the lack of a mutated  $\gamma$ -chain

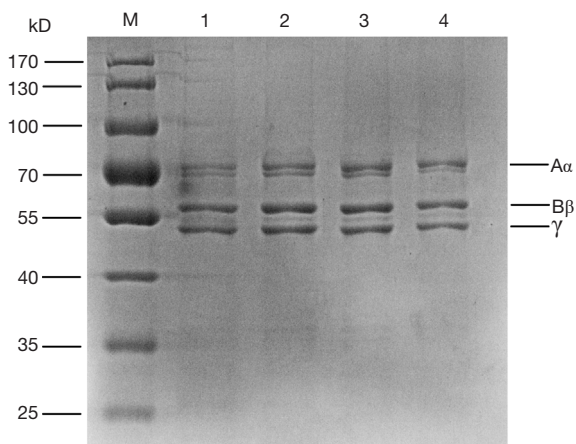


**Figure 2** Sodium dodecylsulfate-polyacrylamide gel electrophoresis analysis of purified fibrinogen isolated from the proband and her family members. Lane 1: healthy control, lane 2: father, lane 3: mother, lane 4: proband.

in the circulating fibrinogen of the proband.

### Pathogenicity analysis and protein modeling of mutant amino acids

Analysis using Mutation Taster software showed that the FG3 c.1094delG variant was neither found in ExAC nor 1000G. The results of the PhastCons and phyloP scores showed that this mutation site was highly conserved.  $\gamma$ 365Cys is located in the  $\gamma$ D-domain of the carboxyl-terminal (C-terminal) portion of the fibrinogen molecule and is paired with  $\gamma$ 352Cys to form the  $\gamma$ 352Cys- $\gamma$ 365Cys intrachain disulfide bond (*Figure 3A*, the yellow area indicated by the thin arrow). There are several critical functional structures that reside in  $\gamma$ 365Cys to the following amino acid sequence in the  $\gamma$ D-domain (*Figure 3A*: residues 365Cys to 437Val are shown in gray). These include hole, which is the critical E:D binding site of fibrinogen molecules; the Gly-Pro-Arg-Pro acetate (GPRP) binding site (GPRP is a fibrin polymerization inhibitor that inhibits the interaction of fibrinogen with the platelet membrane glycoprotein IIb/IIIa complex) (11); and binding sites with the amino end of another fibrinogen A chain (residues 400Thr to 422Glu). As a result of the p. Cys365Phefs\*41 mutation, the  $\gamma$ D-domain structure of the fibrinogen molecule is changed, in that 33 amino acids are deleted (*Figure 3B*: the truncated peptide chain is shown in gray). The disulfide bond of  $\gamma$ 352Cys- $\gamma$ 365Cys

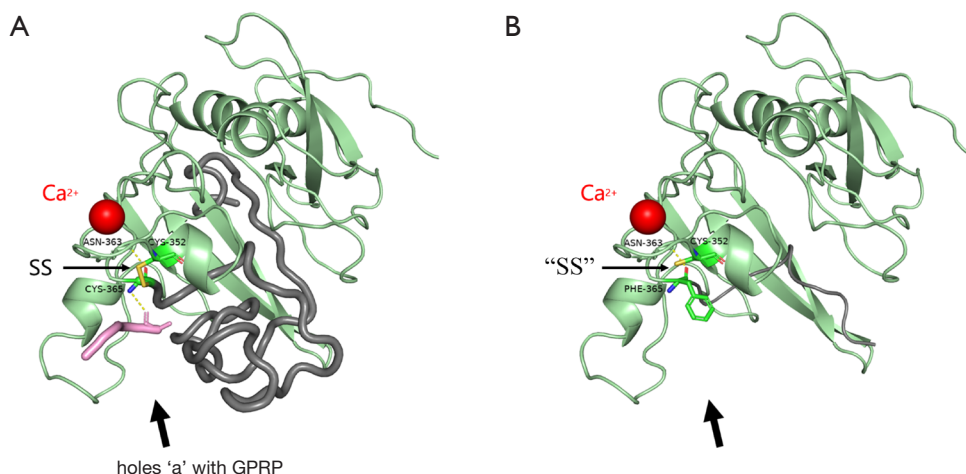


**Figure 3** Fibrinogen molecule structure. (A) Wild type: the thin arrow points to the disulfide bond of  $\gamma$ 352Cys- $\gamma$ 365Cys (expressed as SS), and the thick arrow points to hole a with GPRP. Residues 365Cys to 437Val are shown in gray. (B) Mutant type: the thin arrow points to the broken disulfide bond of  $\gamma$ 352Cys- $\gamma$ 365Cys (expressed as SS) and the thick arrow points to vanishing hole a with GPRP. Truncated peptide chain is shown in gray. GPRP, Gly-Pro-Arg-Pro acetate.

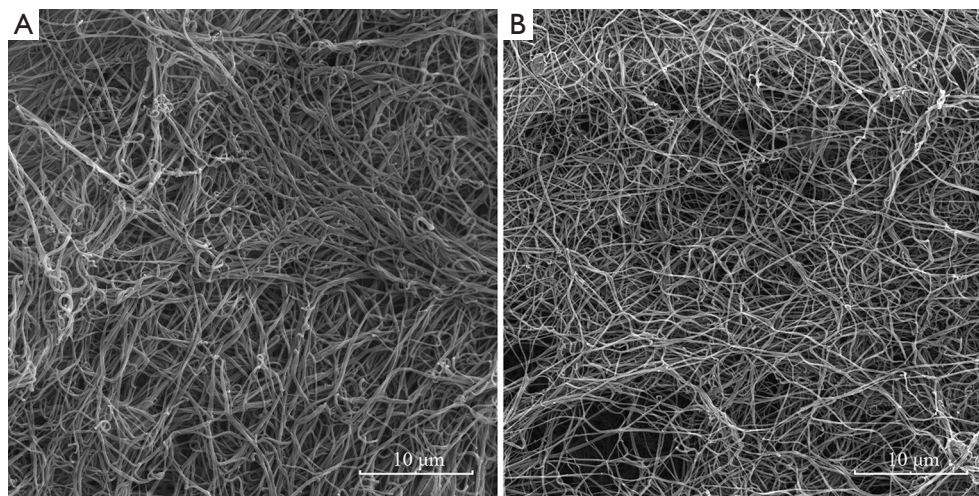


**Figure 4** Scanning electron micrograph of the fibrin network. (A) Healthy control; (B) proband.

becomes disrupted (*Figure 3B*: indicated by the thin arrow), and hole a are destroyed (*Figure 3B*: marked by the thick arrow). Moreover, the shortened peptide chain might affect the functions of the protein and cause nonsense-mediated mRNA decay (NMD).

### SEM

The proband had a complete fibrin network, but the structure was looser than that observed in healthy controls; large pores inside the network formed (*Figure 4A,4B*). The fibers were of uniform thickness, and the mean diameter of the fibers in the fibrin network was  $173\pm 40$  nm, whereas that of the normal fibrin network was  $258\pm 59$  nm. Variance analysis revealed that the mean fiber diameter of the proband's fibrin network was significantly different from that of a normal fibrin network ( $P<0.05$ ).

### Thromboelastography (TEG)

Kaolin-activated thromboelastography has several essential parameters. The R-value indicates the activity of the coagulation factor, the K-value and the  $\alpha$  angle is the rate of fibrin clot formation and reinforcement, and mainly reflect the function and level of fibrinogen, respectively, and the maximum amplitude (MA) value reflects the maximum strength of the blood clot. The coagulation index (CI) value assesses the risk of bleeding. In the proband and her mother, who were both carriers of the mutation, there was

a slight prolongation and reduction of the K-values and the  $\alpha$  angles, which were 4.9 and 3.8 (normal reference range: 1–3 min) and as 43.9 and 47.3 (normal reference range:  $53\text{--}72^\circ$ ), respectively. The proband and her mother's MA were 42.7 and 49.2 mm (normal reference range: 50–70 mm), respectively.

These results showed that the levels of functional fibrinogen, rates of fibrogenesis and reinforcement were down-regulated. and the strength of the blood clots decreased in the 2 carriers. The CI of the proband and her mother were  $-4.2$  and  $-3.2$  (normal reference range: from  $-3$  to  $3$ ), respectively, indicating they had a low coagulation state. The TEG results of younger brother were normal. All other parameters are shown in *Table 4*. According to the above results, the degree of fibrinogen function impairment is related to the fibrinogen concentration.

### CWA

The CWA parameters of the family's healthy members, including the time to reach the fibrinogen threshold, first derivative, second derivative, and delta of the TT test, were all the same. The time to reach the fibrinogen threshold seen in the 2 mutation carriers were significantly longer and their parameters of the TT test were significantly lower. There was a positive correlation with the defect degree of the fibrinogen levels, that is, the lower levels of fibrinogen were a direct result of a longer time to reach the fibrinogen threshold and decreased in the other parameters measured (*Table 5*).

**Table 4** Thromboelastography of the family members

Family member	R (min)	K (min)	$\alpha$ angle ( $^{\circ}$ )	MA (s)	CI
Mother	5.6	3.8	47.3	49.2	-3.2
Proband	4.8	4.9	43.9	42.7	-4.2
Brother	7.0	2.8	54.5	59.8	-2.0
Reference range	5-10	1-3	53-72	50-70	-3 to 3

$\alpha$  angle, slope between R and K; CI, coagulation index; K, kinetics; MA, maximum amplitude; R, reaction time.

**Table 5** Clot waveform analysis of the family members

Family member	Father	Brother	Mother	Proband
First derivative TT, mAbs/s	126.0	128.8	66.2	44.9
Second derivative TT, mAbs/s <sup>2</sup>	348.0	342.2	157.2	101.9
Delta TT, mAbs	246.0	258.9	179.4	94.6
Threshold fibrinogen, s	15.1	15.9	22.3	29.2
Fibrinogen (Clauss assay), g/dL	2.67	2.18	1.61	1.17

TT, thrombin time.

## Discussion

We identified a new heterozygous frameshift mutation in FGG, leading to hypofibrinogenemia in a Chinese family. DNA sequencing revealed a heterozygous mutation in c.1094delG in exon 8 of FGG, resulting in p. Cys365Phefs\*41 (containing a signal peptide) in the proband and her mother. Hypofibrinogenemia is a quantitative fibrinogen disorder. According to the mutation database of fibrinogenic variants (<http://site.geht.org/base-de-donnees-fibrinogene/>), missense mutations are most common in cases of hypofibrinogenemia (11). However, frameshift mutations in FGG genes are rare, which mainly results in quantitative fibrinogen disorders. Several molecular mechanisms of quantitative fibrinogen disorders have been reported, such as defects in synthesis, assembly, or secretion of the protein (12). These defects are often caused by changes in the essential functional structure of the fibrinogen molecule. For example, the 29 disulfide bonds within the molecule are critical for fibrinogen synthesis, secretion, stability. Disulfide bond cleavage is known to impact severely on fibrinogen assembly and secretion (4).

Clinical features in hypofibrinogenemia are highly consistent with fibrinogen activity levels. Most hypofibrinogenemia patients are asymptomatic, but there is a greater risk of bleeding problems or trauma during and after pregnancy (13). Studies have shown that a fibrinogen

activity level above 1.0 g/L can be asymptomatic, and an activity level below 0.7 g/L will cause spontaneous bleeding (12). Fibrinogen replacement therapy can effectively prevent and treat bleeding (14,15). In the present study, the proband had been aware of a predisposition to bleeding, such as hypermenorrhea, gingival bleeding, and slow healing of wounds. Routine blood coagulation tests found that fibrinogen activity and antigen levels decreased, and PT, APTT, and TT were normal in the proband.

Several studies have shown a non-significant difference in the amplitudes and the maximal velocities of coagulation curves in the plasma of patients with fibrinogen quality defects, as well as in normal controls, but patients with fibrinogen quantity defects had lower amplitudes of coagulation curves (16). In the present study, we also noticed that the amplitude was directly related to the amount of fibrinogen in the sample. The lower the fibrinogen levels, the lower the TT test parameters, including the maximum velocity (first derivative) and acceleration (second derivative) of clot formation, as well as the amplitude of the coagulation curve in the family members. The fibrinogen Clauss assay is related to the rate of the reaction, which means the quicker the sample clots, the higher the amount of fibrinogen obtained. The period of time to reach the fibrinogen threshold seen in the 2 mutation carriers was significantly longer, which indicated a decrease in fibrinogen

levels and the ability to form blood clots. Similar results were detected with thromboelastography. The fibrinogen levels were 2.18, 1.61, and 1.17 g/L; the MA values were 59.8, 49.2, and 42.7 s; and the CI values were -2.0, -3.2, and -4.2, respectively, for the younger brother, mother, and proband. These measurements indicated that the blood clots would gradually be weakened, and the risk of bleeding would increase as the levels of fibrinogen decreased.

Studies have shown that tPAIC, TM, TAT, and PIC are all produced in the initial stages of the anticoagulant system response, which can be used to monitor the anticoagulant system activation *in vivo* (17). The results for these measurements were normal in all the family members. The coagulation factors VIII, IX, XI, and XII were also normal in the proband and both her parents. These indicated that the blood coagulation system in these family members was not activated, and the body had a balance between bleeding and coagulation. Because the proband's fibrinogen level was the lowest in her family, she was asymptomatic, but was more prone to bleeding during menstruation and trauma than her mother.

The fibrinogen Clauss/PT-derived ratios of the proband and her mother were 0.7 and 0.72, respectively. It is difficult to determine the defect type using our previous criteria (the cut-off value for this was set at 0.7) (18). Therefore, the purified fibrinogen from the proband, her mother, and her father's plasma was analyzed by SDS-PAGE and found to be normal A $\alpha$ -, B $\beta$ -, and  $\gamma$ -chain patterns were seen. HPLC-MS indicated no mutated  $\gamma$ -chain in the circulating fibrinogen of the proband. Therefore, the patients in this family had varying degrees of fibrinogen quantitative deficiency that was expressed as the clinical phenotype.

The major factors affecting the structure of the fibrin network are fiber thickness, branching, and network density (19). The proband had a complete fibrin network, but the structure was looser than healthy controls, and there were large pores inside the networks, which was probably related to the decrease in fibrinogen concentration observed in the proband. Protein modeling showed that mutations could destroy key D:E binding structures within the fibrinogen molecule, such as hole a, the GPRP binding site, and the binding region to the  $\alpha$ -chain of other fibrinogen molecules. If there were mutated fibrinogen molecules in plasma, then the fibrin network would change abnormally.

In Fibrinogen Tokyo II ( $\gamma$ Arg301Cys), the diameters of the fibers were normal and the nodes extended out from several fiber branches with different lengths and sharp tails. Therefore it is unlikely that the fibers connected to form

the large pores (20). In Fibrinogen Tokyo V ( $\gamma$ Ala327Thr), the diameters of the fibers were small with a large number of fiber nodes and branches. However, the fiber nodes had many broken tails with macro-pores appearing in the network, and the surrounding fibers were entangled (21). Because the D:E and D:D binding between fibrinogen molecules was damaged, which seriously interfered with the horizontal and lateral cross-linking between protein monomers, the polymerization of fiber filaments was terminated in the early stages and could not continue to extend (22). Moreover, the loose network structure most likely increased its permeability to lytic enzymes (19), which means any blood clots formed would be more likely to breakdown, and the risk of bleeding markedly increased.

Pathogenicity analysis and protein modeling of mutant amino acids were performed to better understand the molecular abnormalities of the fibrinogen defects. The mutation is located in the conserved carboxyl terminus of fibrinogen, and paired with  $\gamma$ 352Cys to form the  $\gamma$ 352Cys- $\gamma$ 365Cys intrachain disulfide bond. Previous studies have shown that this disulfide bond has a crucial role in maintaining the tertiary structure of the  $\gamma$ D-domain of the C-terminal domain (23). Site-directed mutagenesis tests showed that disruption of  $\gamma$ 352Cys- $\gamma$ 365Cys allows fibrinogen assembly, but completely blocks secretion of the molecule from CV-1 in Origin Simian-1 (COS-1) cells (23). However, the effects of the mutations on the human body are more complex. When combined with naturally occurring heterozygous cases of  $\gamma$ Cys326Tyr and  $\gamma$ Cys326Ser and their results, Haneishi *et al.* suggested that small amounts of variants might be secreted into plasma (24). So far, 2 heterozygous cases of 2 fibrinogen variants at  $\gamma$ Cys365 substituted by Ser or Asp have been reported, and these caused hypofibrinogenemia and hypodysfibrinogenemia, respectively (25,26).

Obstacles in fibrinogen secretion result in the accumulation of mutated peptide chains in hepatocytes strongly predisposes the development of varying degrees of severe chronic liver disease (27). In the present study, clinically, normal liver function in patients indicates that although fibrinogen secretion is impaired, mutant peptide chains are less likely to accumulate in liver cells. Because the mutation led to the amino acids from  $\gamma$ 365Cys to the subsequent amino acids being completely replaced, and the peptide chain was truncated. This included a vital amino acid,  $\gamma$ 387Ile (excluded in the signal peptide), which is essential for the assembly and secretion of fibrinogen (28). Truncated peptide chains can lead to

NMD, which is an intracellular quality control mechanism that prevents the production of potentially toxic truncated proteins by identifying and degrading transcripts containing translational-termination codons (29).

## Conclusions

We report a novel frameshift mutation in the C-terminal domains of the  $\gamma$ -chain in patients with hypofibrinogenemia with bleeding complications, which has been named “fibrinogen Baise II”. The mutation induces a structural change at the C-terminal of the fibrinogen molecule, resulting in dysfunctional fibrinogen secretion. The risk of bleeding in patients was associated with the degree of fibrinogen defect. Pathogenicity analysis and protein modeling of mutant amino acids will contribute to a better understanding of the molecular pathogenesis of hypofibrinogenemia. The limitation of our study is that there is not large numbers of patients under detecting.

## Acknowledgments

The authors thank the patients and family members for their interest in, and support of, this study. This study received non-financial support from the Clinical Laboratory Center of the First Affiliated Hospital of Jinan University, the Clinical Laboratory of the First Affiliated Hospital of Guangxi Medical University, and the People’s Hospital of Baise, China. The authors are grateful to Dr. Dev Sooranna of Imperial College London for the English language edit.

**Funding:** This research was supported by grants from the National Natural Science Foundation of China (No. 81800130), the Youjiang Medical University for Nationalities of China program (No. yy2020ky062), and the Guangxi Key Research and Development Foundation (Grant No. AB18221029).

## Footnote

**Reporting Checklist:** The authors have completed the MDAR reporting checklist. Available at <https://dx.doi.org/10.21037/atm-21-3207>

**Data Sharing Statement:** Available at <https://dx.doi.org/10.21037/atm-21-3207>

**Conflicts of Interest:** All authors have completed the ICMJE uniform disclosure form (available at <https://dx.doi.org/10.21037/atm-21-3207>).

[org/10.21037/atm-21-3207](https://dx.doi.org/10.21037/atm-21-3207)). The authors have no conflicts of interest to declare.

**Ethical Statement:** The authors are accountable for all aspects of the work in ensuring that questions related to the accuracy or integrity of any part of the work are appropriately investigated and resolved. All procedures performed in this study involving human participants were in accordance with the Declaration of Helsinki (as revised in 2013). The study was approved by the medical ethics committee at the First Affiliated Hospital of Guangxi Medical University, Nanning, Guangxi, China (No. 2020 KY-E-162) and informed consent was taken from all the patients.

**Open Access Statement:** This is an Open Access article distributed in accordance with the Creative Commons Attribution-NonCommercial-NoDerivs 4.0 International License (CC BY-NC-ND 4.0), which permits the non-commercial replication and distribution of the article with the strict proviso that no changes or edits are made and the original work is properly cited (including links to both the formal publication through the relevant DOI and the license). See: <https://creativecommons.org/licenses/by-nc-nd/4.0/>.

## References

1. de Moerloose P, Casini A, Neerman-Arbez M. Congenital fibrinogen disorders: an update. *Semin Thromb Hemost* 2013;39:585-95.
2. Paraboschi EM, Duga S, Asselta R. Fibrinogen as a Pleiotropic Protein Causing Human Diseases: The Mutational Burden of A $\alpha$ , B $\beta$ , and  $\gamma$  Chains. *Int J Mol Sci* 2017;18:2711.
3. Medved L, Weisel JW. Recommendations for nomenclature on fibrinogen and fibrin. *J Thromb Haemost* 2009;7:355-9.
4. Zhang JZ, Redman CM. Role of interchain disulfide bonds on the assembly and secretion of human fibrinogen. *J Biol Chem* 1994;269:652.
5. Weisel JW, Litvinov RI. Fibrin Formation, Structure and Properties. *Subcell Biochem* 2017;82:405-56.
6. Mosesson MW, Siebenlist KR, Meh DA. The structure and biological features of fibrinogen and fibrin. *Ann N Y Acad Sci* 2001;936:11-30.
7. Spraggon G, Everse SJ, Doolittle RF. Crystal structures of fragment D from human fibrinogen and its crosslinked counterpart from fibrin. *Nature* 1997;389:455-62.

8. Doolittle RF. Determining the crystal structure of fibrinogen. *J Thromb Haemost* 2004;2:683-9.
  9. Lounes KC, Ping L, Gorkun OV, et al. Analysis of engineered fibrinogen variants suggests that an additional site mediates platelet aggregation and that "B-b" interactions have a role in protofibril formation. *Biochemistry* 2002;41:5291-9.
  10. Ruberto MF, Marongiu F, Mandas A, et al. The venous thromboembolic risk and the clot wave analysis: a useful relationship? *Clin Chem Lab Med* 2018;56:448-53.
  11. Casini A, Blondon M, Tintillier V, et al. Mutational Epidemiology of Congenital Fibrinogen Disorders. *Thromb Haemost* 2018;118:1867-74.
  12. Neerman-Arbez M, Casini A. Clinical Consequences and Molecular Bases of Low Fibrinogen Levels. *Int J Mol Sci* 2018;19:192.
  13. Casini A, de Moerloose P, Neerman-Arbez M. Clinical Features and Management of Congenital Fibrinogen Deficiencies. *Semin Thromb Hemost* 2016;42:366-74.
  14. Casini A, de Moerloose P. Fibrinogen concentrates in hereditary fibrinogen disorders: Past, present and future. *Haemophilia* 2020;26:25-32.
  15. Zhou W, Luo M, Yan J, et al. A novel fibrinogen gamma-chain mutation, p.Cys165Arg, causes disruption of the gamma165Cys-Bbeta227Cys disulfide bond and ultimately leads to hypofibrinogenemia. *Thromb Res* 2018;172:128-34.
  16. Jacquemin M, Vanlinthout I, Van Horenbeeck I, et al. The amplitude of coagulation curves from thrombin time tests allows dysfibrinogenemia caused by the common mutation FGG-Arg301 to be distinguished from hypofibrinogenemia. *Int J Lab Hematol* 2017;39:301-7.
  17. Mei H, Jiang Y, Luo L, et al. Evaluation the combined diagnostic value of TAT, PIC, tPAIC, and sTM in disseminated intravascular coagulation: A multi-center prospective observational study. *Thromb Res* 2019;173:20-6.
  18. Zhou W, Yan J, Deng D, et al. Diagnosis of congenital dysfibrinogenemia, *Chin J Lab Med* 2020;43:406-10.
  19. Lord ST. Molecular mechanisms affecting fibrin structure and stability. *Arterioscler Thromb Vasc Biol* 2011;31:494-9.
  20. Mosesson MW, Siebenlist KR, Diorio JP, et al. The role of fibrinogen D domain intermolecular association sites in the polymerization of fibrin and fibrinogen Tokyo II (gamma 275 Arg-->Cys). *J Clin Invest* 1995;96:1053-8.
  21. Hamano A, Mimuro J, Aoshima M, et al. Thrombophilic dysfibrinogen Tokyo V with the amino acid substitution of gammaAla327Thr: formation of fragile but fibrinolysis-resistant fibrin clots and its relevance to arterial thromboembolism. *Blood* 2004;103:3045-50.
  22. Sugo T, Endo H, Matsuda M, et al. A classification of the fibrin network structures formed from the hereditary dysfibrinogens. *J Thromb Haemost* 2006;4:1738-46.
  23. Zhang JZ, Redman C. Fibrinogen assembly and secretion. Role of intrachain disulfide loops. *J Biol Chem* 1996;271:30083-8.
  24. Haneishi A, Terasawa F, Fujihara N, et al. Recombinant variant fibrinogens substituted at residues gamma326Cys and gamma339Cys demonstrated markedly impaired secretion of assembled fibrinogen. *Thromb Res* 2009;124:368-72.
  25. Brennan SO, Andrew L, Mark S. Novel FGG variant ( $\gamma$ 339C→S) confirms importance of the  $\gamma$ 326–339 disulphide bond for plasma expression of newly synthesised fibrinogen. *Thromb Haemost* 2015;113:903-5.
  26. Castaman G, Giacomelli SH, Biasoli C, et al. Risk of bleeding and thrombosis in inherited qualitative fibrinogen disorders. *Eur J Haematol* 2019;103:379-84.
  27. Asselta R, Paraboschi EM, Duga S. Hereditary Hypofibrinogenemia with Hepatic Storage. *Int J Mol Sci* 2020;21:7830.
  28. Okumura N, Terasawa F, Tanaka H, et al. Analysis of fibrinogen gamma-chain truncations shows the C-terminus, particularly gammaIle387, is essential for assembly and secretion of this multichain protein. *Blood* 2002;99:3654-60.
  29. Guo WT, Xu WY, Gu MM. Nonsense-mediated mRNA decay and human monogenic disease. *Yi Chuan* 2012;34:935-42.
- (English Language Editor: R. Scott)

**Cite this article as:** Zhou W, Huang Y, Wei J, Wang JL, Huang B, Zhou X, Yan J, Wu Y, Lin F, Wen W. A novel fibrinogen  $\gamma$ -chain frameshift mutation, p. Cys365Phefs\*41, causing hypofibrinogenemia with bleeding phenotype in a Chinese family. *Ann Transl Med* 2021;9(16):1308. doi: 10.21037/atm-21-3207